Insurance Rate Differentiation of Multi-Hazard Shaking-Tsunami Loss Coverage for Subduction Earthquakes

Jie Song
PhD Candidate, Dept. of Civil Engineering, University of Bristol, Bristol, United Kingdom

Katsuichiro Goda
Associate Professor, Dept. of Earth Sciences, University of Western Ontario, London, Canada

ABSTRACT: This study proposes a new method of determining financial exposure and insurance premium rate for multi-hazard earthquake-tsunami risks due to mega-thrust subduction earthquakes. Since tsunami risk is sensitive to site-specific attributes (e.g. elevation, site-to-shoreline distance, and topographical feature), such characteristics of properties should be taken into account to differentiate the insurance premium rates for different policyholders. To investigate this problem, a new performance-based earthquake-tsunami engineering tool is used. Influences of local tsunami-related risk factors on the financial risk exposure as well as insurance premium rates are investigated through a case study that focuses upon building portfolios in Sendai and Onagawa, Miyagi Prefecture, Japan.

1. INTRODUCTION

Recent catastrophic earthquakes and tsunamis have highlighted the importance of financial risk transfer instruments to protect households and businesses from severe economic consequences. In seismic-prone countries, such as Japan, the United States, and New Zealand, earthquake insurance that covers shaking-related damage and loss has been used in practice (Bozza *et al*., 2015; Goda *et al*., 2015). A coastal region threatened by tsunamis is also under seismic risk, since a tsunami is usually triggered by a mega-thrust subduction event. Currently, shaking and tsunami risks are treated as two separate hazards. In setting a fair price for earthquake and tsunami insurance coverage, it is important to evaluate the multi-hazard risks jointly as an accurate assessment of their financial risk exposure is crucial in making underwriting decisions of insurance policies for shaking and tsunami risks.

To develop an insurance rate-making method for multi-hazard shaking-tsunami risk coverage, a new performance-based earthquake-tsunami engineering framework can be adopted (Goda and De Risi, 2018). Although the spatial extent of tsunami damage is limited to coastal regions, tsunami risk can be devastating in extreme situations. Moreover, tsunami risk is particularly sensitive to elevation, distance from the shoreline, and coastal topography (Song *et al*., 2017). It is desirable to differentiate insurance premium rates based on these tsunami-related risk factors. To investigate this problem, two building portfolios in plain and ria coast (Sendai and Onagawa), respectively, in Miyagi Prefecture, Japan are focused upon as a case study. Based on shaking and tsunami vulnerability curves, multi-hazard risks of subduction earthquakes off the Tohoku coast of Japan are assessed using a stochastic earthquake rupture model. The study integrates tsunami risk with seismic risk to derive multi-hazard loss curves and promotes the calculation of equitable premium rates based on the importance of site-specific attributes of a portfolio.

2. EARTHQUAKE-TSUNAMI LOSS MODEL

This section presents main components of the multi-hazard loss estimation framework for cascading shaking and tsunami hazards. The methodology is illustrated in Figure 1. Details of the computational tool can be found in Goda and De Risi (2018).

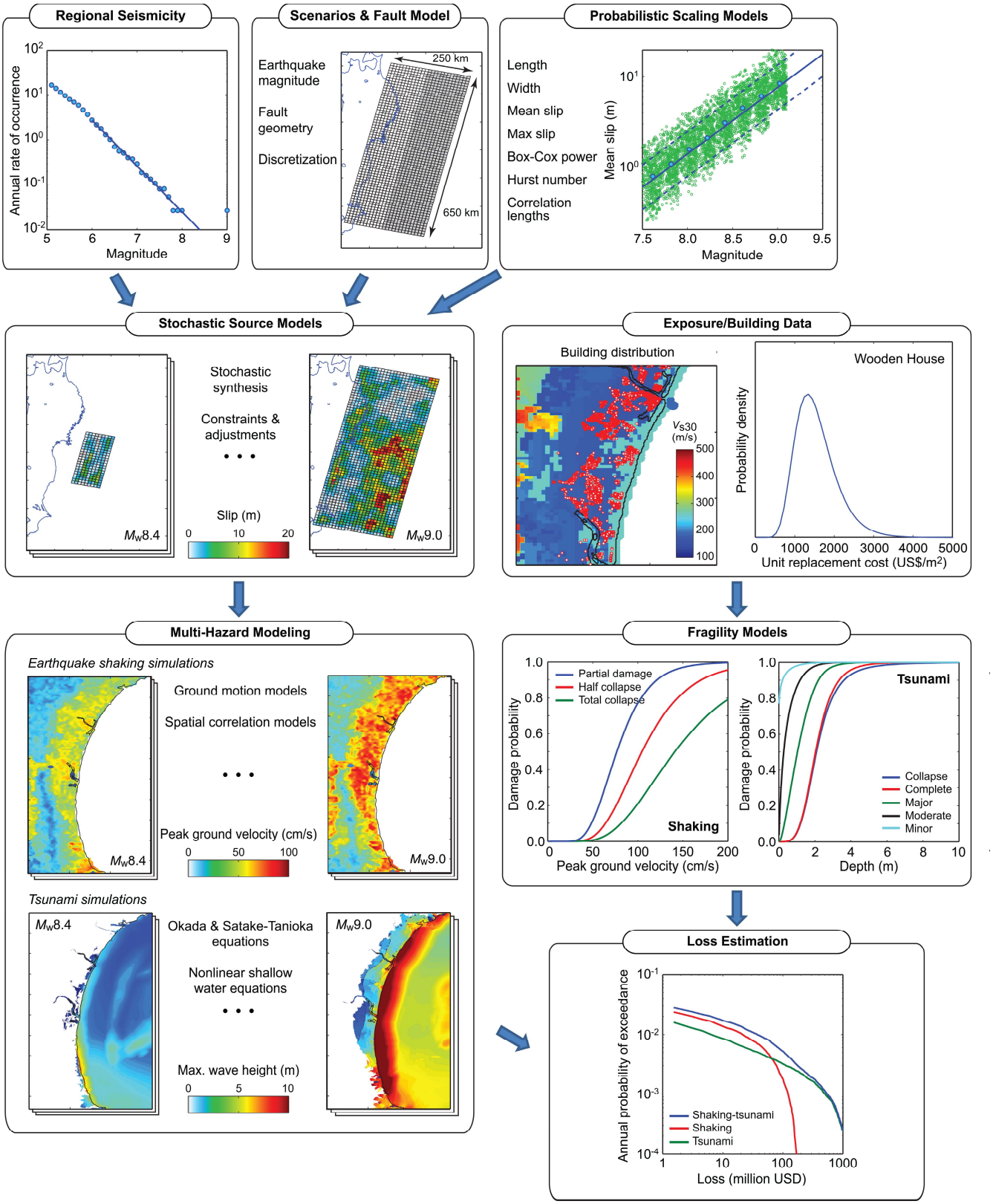

Figure 1: Multi-hazard loss estimation procedure for shaking and tsunami.

Regional seismicity model The expected distribution of earthquake occurrences is characterized in accordance with the seismic hazard model for the Tohoku region proposed by the Headquarters for Earthquake Research Promotion (2013). Using earthquake catalog data in the Tohoku region, the annual occurrence rate of tsunamigenic earthquakes having M_w7.5 is estimated to be 0.08. A Gutenberg-Richter curve is fitted to obtain the recurrence values for events between M_w7.5 and M_w9.1, which are discretized with a 0.2 interval. The return periods of earthquakes with moment magnitudes greater than 7.5, 7.7, 7.9, 8.1, 8.3, 8.5, 8.7, and 8.9 are calculated as 13, 21, 35, 59, 103, 187, 378, and 1,000 years, respectively.

Fault model A regional fault source model is developed by extending the fault plane geometry for the 2011 Tohoku earthquake covering an area of 650 km long by 250 km wide. The strike angle is constant at 193º, while the dip angle is considered variable along the subducting plate interface, gradually steepening from 8º to 16º in the down-dip direction. The eastern boundary of the fault plane model approximately coincides with the Japan Trench. To characterize heterogeneous earthquake slips over the fault plane, the source zone is discretized into sub-faults of 10km by 10km.

Scaling model Eight source parameters are used to characterize the earthquake rupture in terms of fault geometry and slip distribution (Goda *et al*., 2016). The geometrical parameters, i.e. fault width and fault length, determine the size of the fault rupture, and the position of the synthesized fault plane is determined such that it fits within the source zone. The slip parameters, i.e. mean slip and maximum slip, specify the earthquake slip statistics over the fault plane. The Box-Cox power transformation parameter determines how the slip values are marginally distributed over the fault plane and is used to capture non-normal characteristics of earthquake slip (Goda *et al*., 2014). The spatial slip distribution parameters, i.e. correlation length along dip/strike and Hurst number, are used to characterize the heterogeneity of earthquake slip over the fault plane, represented by the von Kármán wavenumber spectrum.

Stochastic source model After sampling the spatial slip distribution parameters, a random slip field is generated using the Fourier integral method (Goda *et al*., 2014), where the amplitude spectrum is represented by the von Kármán spectrum and its phase is uniformly distributed between 0 and 2π. To achieve a slip distribution with realistic heavy-tail features, the synthesized slip distribution is converted via Box-Cox power transformation. The transformed slip distribution is then adjusted to achieve the target mean slip and to avoid very large slip values exceeding the target maximum slip. In total, 4,000 stochastic source models are generated (500 models for each of the eight magnitude ranges).

Ground motion model Seismic intensity measures at building locations are evaluated by using ground motion prediction equations for peak ground velocity (PGV) together with spatial correlation models for prediction errors. Among existing ground motion models, a relationship by Morikawa and Fujiwara (2013) is chosen because it is applicable to mega-thrust interface subduction earthquakes in Japan and the underlying data include strong motion observations from the 2011 Tohoku earthquake. Simulation of PGV random fields is carried out by considering the 250-m grid spacing. The median values at the 250-m grids are evaluated by using the Morikawa-Fujiwara equation, whereas random error terms of the equation are simulated by considering the average spatial correlation model by Goda and Atkinson (2010) and separation distance matrix of the grid points.

Inundation model To obtain inundation depths at building locations, nonlinear shallow water equations are evaluated (Goto *et al.*, 1997) by considering initial water surface elevation due to the earthquake rupture. The computational domains are nested at four grid resolutions: 1350-m, 450-m, 150-m, and 50-m domains (note that land elevation data are represented by 50-m grids). The simulated tsunami wave heights at the

grid points are used to estimate inundation depths at building locations. Inundation simulations are conducted for the 4,000 stochastic sources.

Exposure model The exposure model characterizes the assets at risk within a region of interest. The building dataset used in this study is based on the post-2011-Tohoku tsunami damage data compiled by the Ministry of Land Infrastructure and Transportation (MLIT). The data contain information on building locations, damage levels based on post-tsunami surveys (minor, moderate, extensive, complete, or collapse, as defined by the MLIT), structural material (reinforced concrete, steel, wood, and others), and the number of stories. Regional statistics of unit building costs and floor areas are used to estimate the cost of the buildings, both of which are modeled as lognormal variables.

Fragility model Fragility functions relate hazard intensity measures to probabilities of attaining different damage states. Three empirical shaking fragility models for low-rise wooden buildings are implemented with an equal weight. The models by Yamaguchi and Yamazaki (2001), Midorikawa *et al*. (2011), and Wu *et al*. (2016) differ in underlying shaking damage data from the past earthquakes in Japan. All three models adopt PGV as seismic intensity measure and consider three damage states: partial damage, half collapse, and complete collapse. The corresponding damage ratios are assigned as 0.03–0.2, 0.2–0.5, and 0.5–1.0, respectively. For tsunami, we adopt an empirical fragility model by De Risi *et al.* (2017), which is based on the tsunami damage data gathered by the MLIT and uses inundation depth as intensity measure. According to the MLIT, damage ratios for the minor, moderate, extensive, complete, and collapse damage states are assigned as: 0.03–0.1, 0.1–0.3, 0.3–0.5, 0.5–1.0, and 1.0, respectively. The combined damage state due to shaking and tsunami is determined as the larger of the incurred damage states from the two hazards for a given common event.

Loss model The monetary loss associated with the shaking and tsunami damage on a building is calculated by sampling the total replacement cost from the lognormal distribution and multiplying it by the damage ratio determined from the fragility analysis. The procedure is repeated for all buildings in the portfolio to obtain the total tsunami loss for each event in the stochastic sample. These loss samples can then be used to construct the exceedance probability curves of shaking-tsunami loss. The multi-hazard loss model facilitates the effective risk management of cascading shaking and tsunami due to mega-thrust subduction earthquakes (Goda and De Risi, 2018).

3. APPLICATION: INSURANCE RATE DIFFERENTIATION

Using the developed multi-hazard loss estimation tool, both single-hazard and multi-hazard loss curves for different building portfolios can be developed based on simulation results. In this section, analysis results are employed to evaluate the regional financial exposure to building portfolios and to calculate the insurance premium rates for several buildings having different location/topographical attributes. The insurance premium is typically composed of pure premium, risk premium, and transaction fees. The main focus of this study is on pure premium rate, which can be calculated as average annual loss normalized by total insured amount.

The regional aspects are important for insurance underwriting because the loss characteristics, especially for extreme situations, can be decisive factors. These can be captured through risk metrics, such as value-at-risk and probable maximum loss at selected probability levels (Goda *et al*., 2015). On the other hand, the financial risk for nearly-identical buildings but with different elevations or at different distances from the shoreline can lead to significant differences in pure insurance premium rates. Therefore, insurers may be interested in introducing these as important tsunami-related risk factors to differentiate insurance premiums for the coverage to avoid possible effects due to moral hazard and adverse selection.

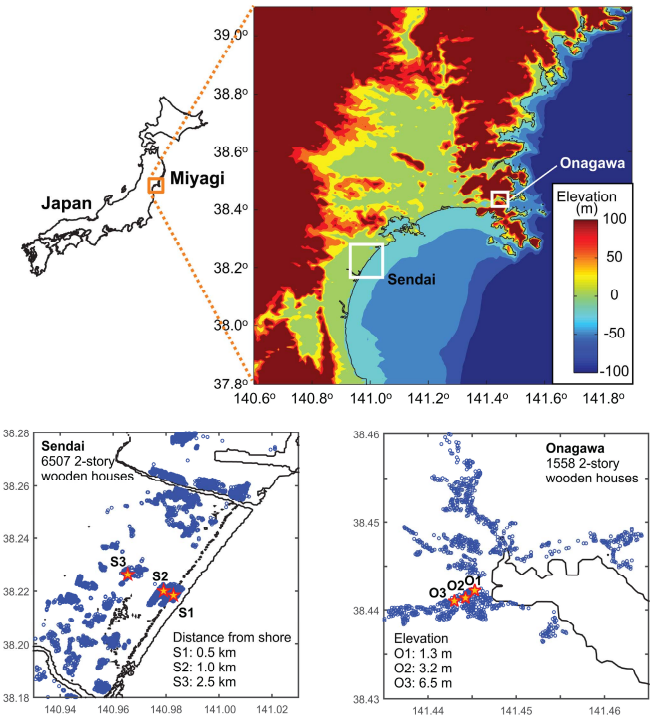

Figure 2: Building distributions in Sendai and Onagawa.

In this study, residential 2-story wooden houses are focused upon. Based on the MLIT database, there are 6,507 and 1,558 houses in the selected areas of Sendai and Onagawa, respectively. Sendai is located in a low-lying coastal plain, while Onagawa is located along ria coast (submerged valleys). The regional topographical map of Miyagi Prefecture is shown in Figure 2. The spatial distributions of the houses in the two areas are also displayed in Figure 2. For the investigations of insurance premium rates as a function of different tsunami-related risk factors, three buildings are selected in each location; they are denoted by S1, S2, and S3 for Sendai and O1, O2, and O3 for Onagawa (see Figure 2 for their locations). The buildings S1 to S3 are at similar elevations of about 2 m above the mean sea level but are at different distances from the shoreline (about 0.5 km, 1.0 km, and 2.5 km). On the other hand, the buildings O1 to O3 are at similar distances from the shoreline (note: the scale for the Onagawa map is much smaller than that for Sendai) but at different elevations (about 1.3 m, 3.2 m, and 6.5 m). The site classes for all six sites are soft soil and their site amplification factors for shaking are identical. Based on this set-up, the effects of site-to-shoreline distances and elevations as well as the topographical effects (i.e. Sendai versus Onagawa) can be examined.

3.1. Regional shaking and tsunami risks

The regional differences of the single-hazard and multi-hazard loss curves are investigated first. Figure 3 shows shaking, tsunami, and shaking&tsunami loss curves for all wooden houses within the selected areas of Sendai and Onagawa. For both locations, shaking risks tend to be dominant at low return periods (less than a few hundred years), whereas tsunami risks increase rapidly with the return period.

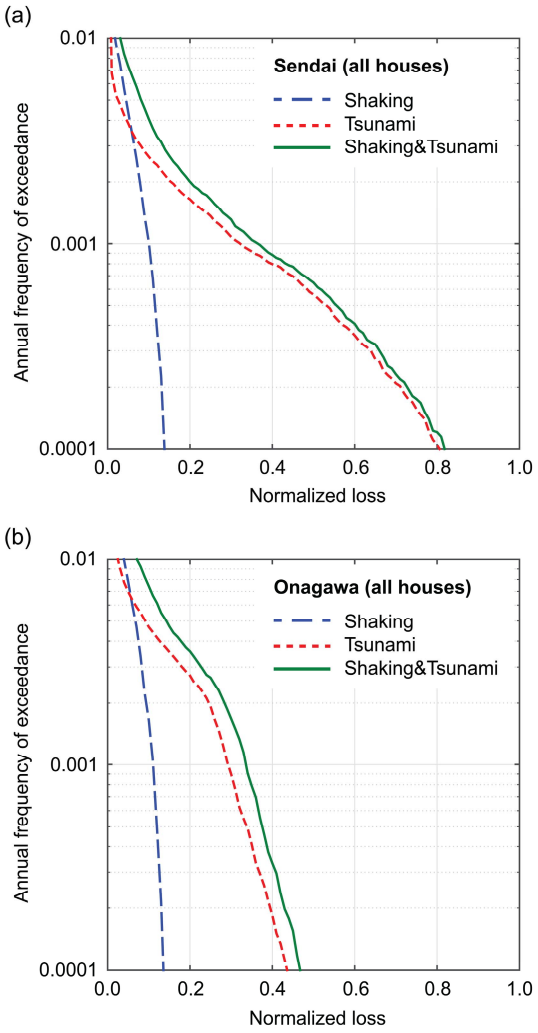

Figure 3: Shaking-tsunami loss curves for (a) Sendai and (b) Onagawa.

The shaking risks in Onagawa are generally greater than those in Sendai at shorter return periods, but they become closer at longer return periods. This is because Onagawa is closer to the rupture zones, but the effects of this difference on shaking risks become negligible for rare cases because the rupture areas tend to be extended towards the land as the magnitude of the earthquake becomes larger. The extreme cases of shaking risks for the building portfolios tend to be capped because of magnitude and distance saturation.

The majority of the houses in Sendai can be completely inundated with significant wave depths (as observed during the 2011 Tohoku event). Consequently, the tsunami risk curve and thus the combined risk curve reach high values of normalized loss (near 0.8) in extreme cases (beyond the return period of 1,000 years). In contrast, the building portfolio in Onagawa includes houses that are at relatively high elevations and thus even in extreme situations, complete devastation of all houses in the portfolio does not occur. It is also important to notice that at intermediate hazard levels (between return periods of 100 and 1,000 years), tsunami risks in Onagawa are higher than those in Sendai due to ria characteristics of the topography.

In terms of pure insurance premiums, the average annual losses for different hazards (both single-hazard and multi-hazard) are calculated and summarized in Table 1 and Table 2 for Sendai and Onagawa, respectively. The results indicate that the premium rates for shaking, tsunami, and shaking&tsunami coverage for Onagawa are greater than those for Sendai. It is also important to note that the rates for tsunami are greater than those for shaking at both locations. This clearly demonstrates that for major subduction earthquakes, tsunami risks cannot be neglected. In this context, it is also interesting to point out that the General Insurance Rating Organization of Japan currently sets the insurance premium rates to 0.1% to 0.2% for covering earthquake damage mainly due to shallow crustal earthquakes for residential buildings in Miyagi Prefecture (see https://www.giroj.or.jp/ratemaking/earthquake/). The above-mentioned rates are uniform within the prefecture and include risk premium as well as transaction costs. Assuming that the calculated insurance rates for multi-hazard coverage due to major subduction events are reasonable, the contributions of tsunami risk caused by subduction earthquakes are significant. These are important results from this study because the risks due to very large subduction earthquakes in Japan are not fully incorporated in the financial risk calculations.

Table 1: Normalized average annual loss for buildings in Sendai.

	Shaking (%)	*Tsunami (%)*	*Shaking-tsunami (%)*
All buildings	*0.063*	*0.106*	*0.164*
S1	*0.032*	*0.183*	*0.210*
S2	*0.027*	*0.075*	*0.100*
S3	*0.036*	*0.022*	*0.058*

Table 2: Normalized average annual loss for buildings in Onagawa.

	Shaking (%)	*Tsunami (%)*	*Shaking-tsunami (%)*
All buildings	*0.102*	*0.143*	*0.234*
O1	*0.126*	*0.801*	*0.873*
O2	*0.119*	*0.319*	*0.414*
O3	*0.116*	*0.141*	*0.248*

3.2. Insurance rate differentiation for buildings in Sendai and Onagawa

Tsunami risks significantly vary in space. The key factors for such variations include: local elevation, distance from the shoreline, and coastal topography (Song *et al.*, 2017). To evaluate the single as well as multi-hazard losses for individual buildings having different features, two sets of three houses are considered (Figure 2).

Figure 4 and Figure 5 show the shaking-tsunami loss curves for S1, S2, and S3 buildings in Sendai and O1, O2, and O3 buildings in Onagawa, respectively. The shaking risk curves for S1, S2, and S3 or for O1, O2, and O3 do not vary significantly (note: the shaking loss curves for Onagawa are greater than those for Sendai, as discussed in Section 3.1). In contrast, the tsunami

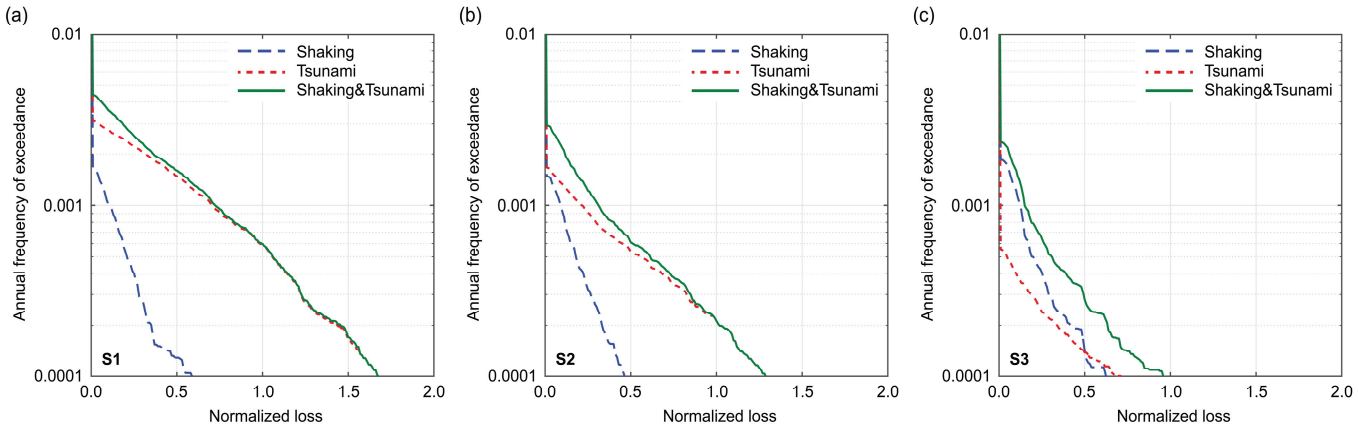

Figure 4: Shaking-tsunami loss curves for Sendai: (a) S1, (b) S2, and (c) S3.

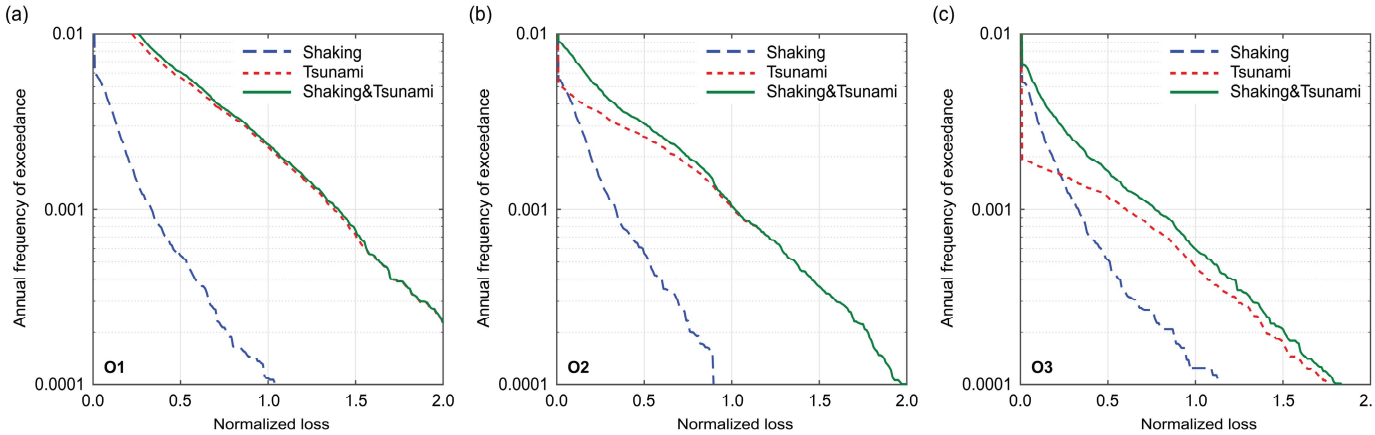

Figure 5: Shaking-tsunami loss curves for Onagawa: (a) O1, (b) O2, and (c) O3.

risk curves and thus the combined risk curves change significantly, depending on the building sites. Typically, the tsunami risks decrease from S1 to S3 due to increased distances to the shoreline and from O1 to O3 due to increased elevations. The visual inspections of the loss curves indicate that the effects of these local building characteristics are remarkable. It is also important to note that the tsunami risks for S1 and O1 (i.e. similar elevation and distance to the shoreline but different regional topography) are significantly different.

To quantify the effects of different tsunami-related risk factors on the pure premium rates, the average annual losses for the six individual buildings are calculated and summarized in Tables 1 and 2. The premium rates for shaking risks are consistent across S1 to S3 and O1 to O3 Note that the rates for S1 to S3 are smaller than the regional average for Sendai. This is because of the differences of the local site conditions; the majority of the buildings in Sendai are on softer sites than the selected building sites. The pure premium rates for tsunami risks depend significantly on the tsunami-related risk factors. For instance, the rate for S1 is 8 to 9 times greater than that for S3 (i.e. site-to-shoreline distance effect), whereas the rate for O1 is 5 to 6 times greater than that for O3 (i.e. elevation effect). The rates for the individual buildings differ significantly from the regional average which can be considered as the premium rate when no rate differentiation scheme is implemented. These comparisons indicate that the local tsunami risk levels vary depending on site-specific features and the risk factors considered may be useful for more detailed insurance rate-making schemes. It is also important to point out that the risk factors that are discussed in this study can be obtained relatively easily from high-resolution digital

elevation models for the areas. Therefore, significant data collection from the insured properties is not necessary.

4. CONCLUSIONS

A new insurance rate-making method for multi-hazard shaking-tsunami risk coverage was developed and was applied to a realistic case study in Sendai and Onagawa, Miyagi Prefecture, Japan. The developed tool facilitates the evaluation of regional financial exposure to both ground shaking and tsunami, and can be used to calculate the insurance premium rates for buildings having different location/topographical attributes. The tsunami-related risk factors, such as elevation, distance from the shoreline, and topograhyical feature, were found to be signfiicant. It is possible to implement the insurance rate differentiation based on these factors because they can be derived from digital elevation models.

5. ACKNOWLEDGEMENTS

This work is supported by the Leverhulme Trust (RPG-2017-006) and the Canada Research Chair in Multi-Hazard Risk Assessment program at Western University (950-232015).

6. REFERENCES

Bozza, A., Asprone, D., and Manfredi, G. (2015). Developing an integrated framework to quantify resilience of urban systems against disasters. *Natural Hazards*, 78, 1729–1748.

De Risi, R., Goda, K., Yasuda, T., and Mori, N. (2017). Is flow velocity important in tsunami empirical fragility modeling?, *Earth-Science Review*, 166, 64–82.

Goda, K., and Atkinson, G.M. (2010). Intraevent spatial correlation of ground-motion parameters using SK-net data. *Bulletin of the Seismological Society of America*, 100(6), 3055–3067.

Goda, K., Mai, P.M., Yasuda, T., and Mori, N. (2014). Sensitivity of tsunami wave profiles and inundation simulations to earthquake slip and fault geometry for the 2011 Tohoku earthquake. *Earth, Planets and Space*, 66, 105.

Goda, K., Wenzel, F., and Daniell, J. (2015). Insurance and reinsurance models for earthquake. In: *Encyclopedia of Earthquake Engineering* (M. Beer, E. Patelli, I. A. Kougioumtzoglou, S. K. Au, eds.), Springer.

Goda, K., Yasuda, T., Mori, N., and Maruyama, T. (2016). New scaling relationships of earthquake source parameters for stochastic tsunami simulation. *Coastal Engineering Journal*, 58, 1650010.

Goda, K., and De Risi, R. (2018). Multi-hazard loss estimation for shaking and tsunami using stochastic rupture sources. *International Journal of Disaster Risk Reduction*, 28, 539–554.

Goto, C., Ogawa, Y., Shuto, N., and Imamura, F. (1997). Numerical method of tsunami simulation with the leap-frog scheme, IOC Manual, UNESCO, No. 35, Paris, France.

Headquarters for Earthquake Research Promotion (2013). Investigations of future seismic hazard assessment, 217 p.

Midorikawa, S., Ito, Y., and Miura, H. (2011). Vulnerability functions of buildings based on damage survey data of earthquakes after the 1995 Kobe earthquake. *Journal of Japan Association for Earthquake Engineering*, 11(4), 34–47.

Ministry of Land Infrastructure and Transportation (MLIT) (2014). Survey of tsunami damage condition. http://www.mlit.go.jp/toshi/toshi-hukkou-arkaibu.html.

Morikawa, N., and Fujiwara, H. (2013). A new ground motion prediction equation for Japan applicable up to M9 mega-earthquake. *Journal of Disaster Research*, 8(5), 878–888.

Song, J., De Risi, R., and Goda, K. (2017). Influence of flow velocity on tsunami loss estimation. *Geosciences*, 7(4), 114.

Wu, H., Masaki, K., Irikura, K., and Kurahashi, S. (2016). Empirical fragility curves of buildings in northern Miyagi Prefecture during the 2011 off the Pacific coast of Tohoku earthquake. *Journal of Disaster Research*, 11(6), 1253–1270.

Yamaguchi, N., and Yamazaki, F. (2001). Estimation of strong motion distribution in the 1995 Kobe earthquake based on building damage data. *Earthquake Engineering & Structural Dynamics*, 30(6), 787–801.